Supplementary information

Ligand-activated EGFR/MAPK signaling but not PI3K, are key resistance mechanisms to EGFR-therapy in colorectal cancer

Xueping Qu1*, Habib Hamidi1*, Radia M. Johnson1, Ethan S. Sokol 2, Eva Lin 1, Cathy Eng3, Tae Won Kim4, Johanna Bendell5, Smruthy Sivakumar2, Benjamin Kaplan2, Felipe de Sousa e Melo1, Andrew Mancini1, Matthew Wongchenko1, Yi Shi1, David Shames1, Yibing Yan1, Fortunato Ciardiello 6, Carlos Bais1#

1. Genentech, Inc., South San Francisco, CA, USA
2. Foundation Medicine, Inc., Boston, MA, USA
3. MD Anderson Cancer Center, Houston, TX, USA
4. Asan Medical Center, University of Ulsan, Seoul, Korea
5. Sarah Cannon Research Institute/Tennessee Oncology, Nashville, TN, USA
6. Università degli Studi della Campania Luigi Vanvitelli, Naples, Italy.

* These authors contributed equally; # Corresponding author, baiscarlos@gmail.com

Supplementary Figure 1

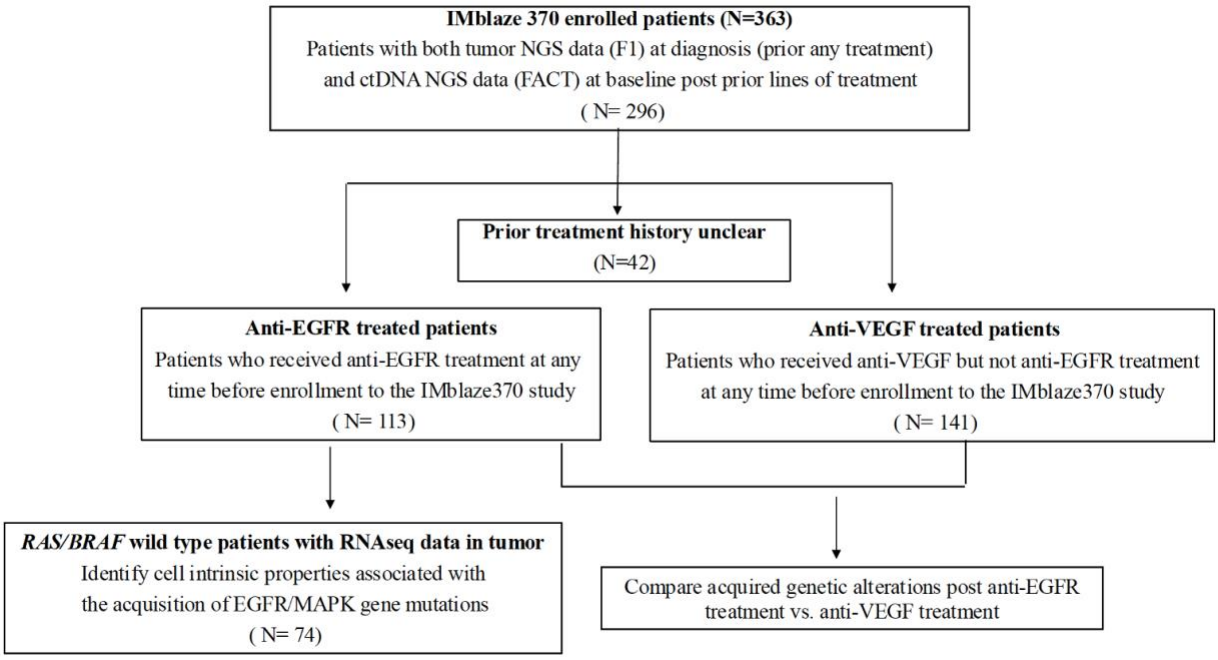

Supplementary Fig. 1. Flow chart of IMblaze 370 enrolled patients and sample selection for analysis. Flow chart showing how patients from the IMblaze370 study were selected for analysis. Patients were grouped based on prior treatment with anti-EGFR or anti-VEGF therapies. A subset of anti-EGFR–treated patients with RNA-seq data and RAS/BRAF wild-type tumors were used to identify intrinsic properties associated with the acquisition of EGFR/MAPK pathway gene mutations.

Supplementary Figure 2

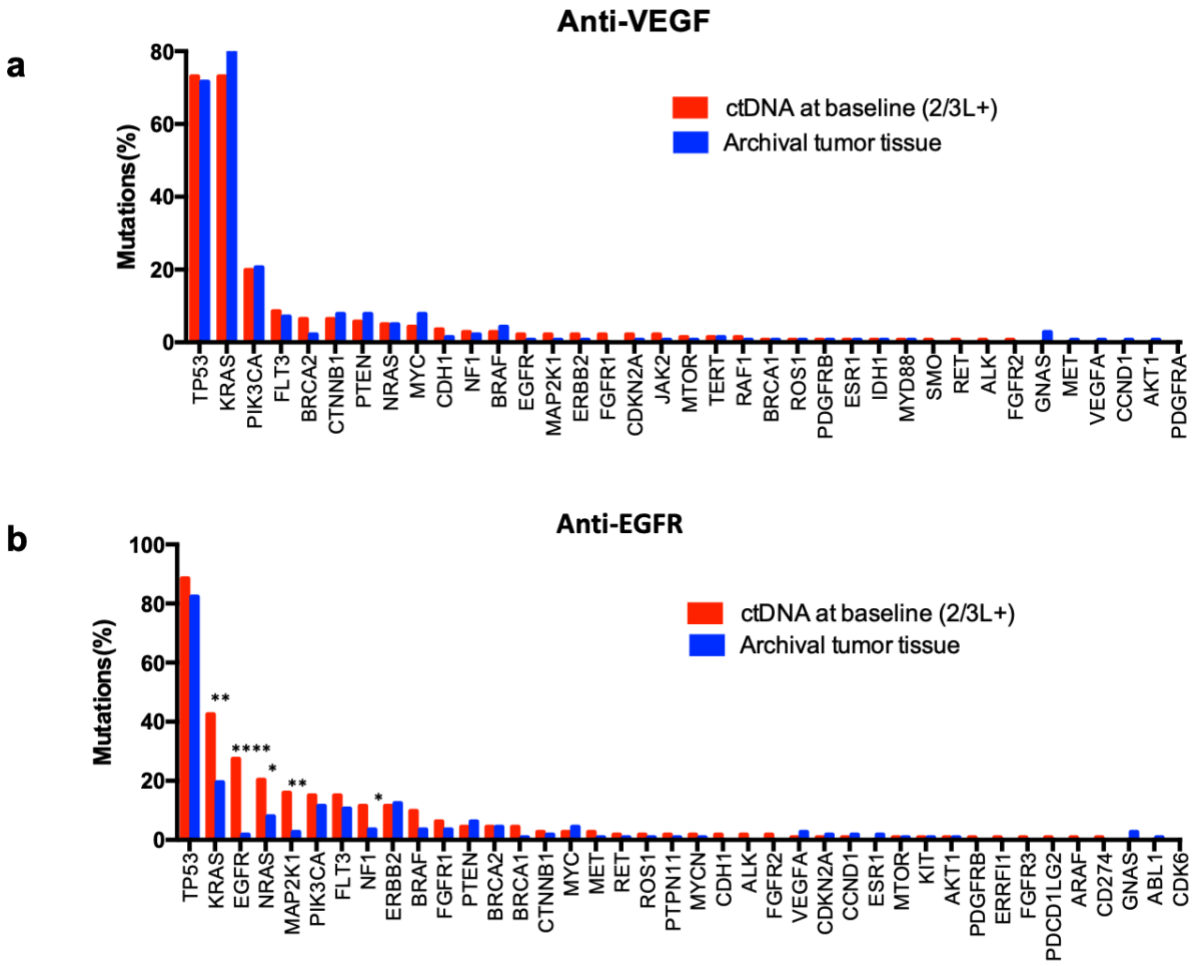

Supplementary Fig. 2. Comparison of genomic alterations detected in plasma samples at baseline (2/3L+) and in archival tissues from IMblaze370 patients. (a) anti-VEGF treated patients (N=141), and (b)anti-EGFR treated patients (N=113). Genes with at least one alteration detected in ctDNA or archival tissue are listed. Only known and likely oncogenic alterations in each gene were considered for the analysis. *P* value determined by two-tailed Fisher's test. ****: *P*<0.00001, ***: *P*<0.0001, **: *P*<0.001, and *: *P*<0.05. Source data for panels a and b are provided as a Source Data file.

Supplementary Figure 3

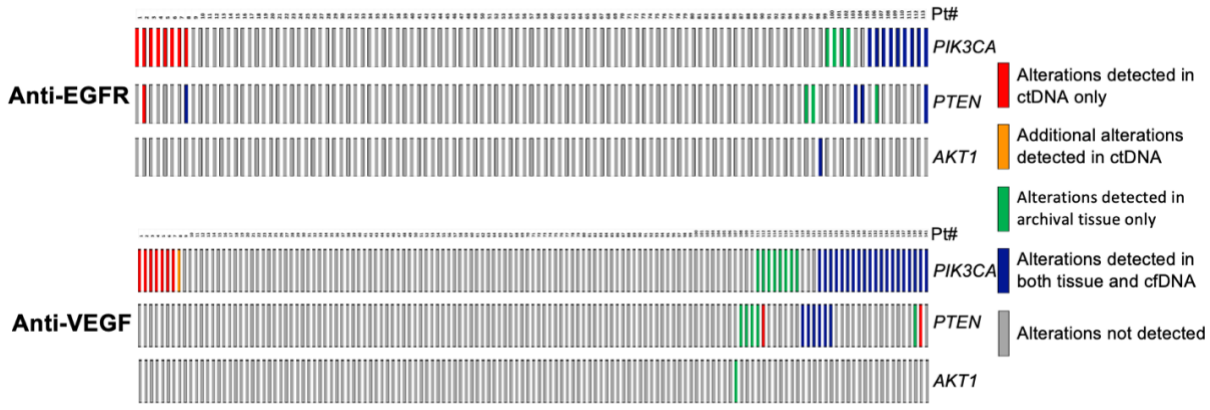

Supplementary Fig. 3. Comparison of PI3K/AKT pathway gene-level alterations identified in paired plasma versus tumor tissue with each pair of bars. Bars in the same column represent an individual patient. Top, Alterations detected in patients that received prior anti-EGFR therapies(N=113). Bottom, alterations detected in patients that received prior anti-VEGF therapies(N=141). Red represents alterations identified in plasma but not in tumor tissue. Orange represents additional alterations identified in plasma compared to those detected in paired archival tumor tissue. Green represents alterations identified in tumor tissue but not in plasma. Blue represents alterations identified in both plasma and tumor tissue. Gray represents no alterations detected in either plasma or tumor tissue. Source data are provided as a Source Data file.

Supplementary Figure 4

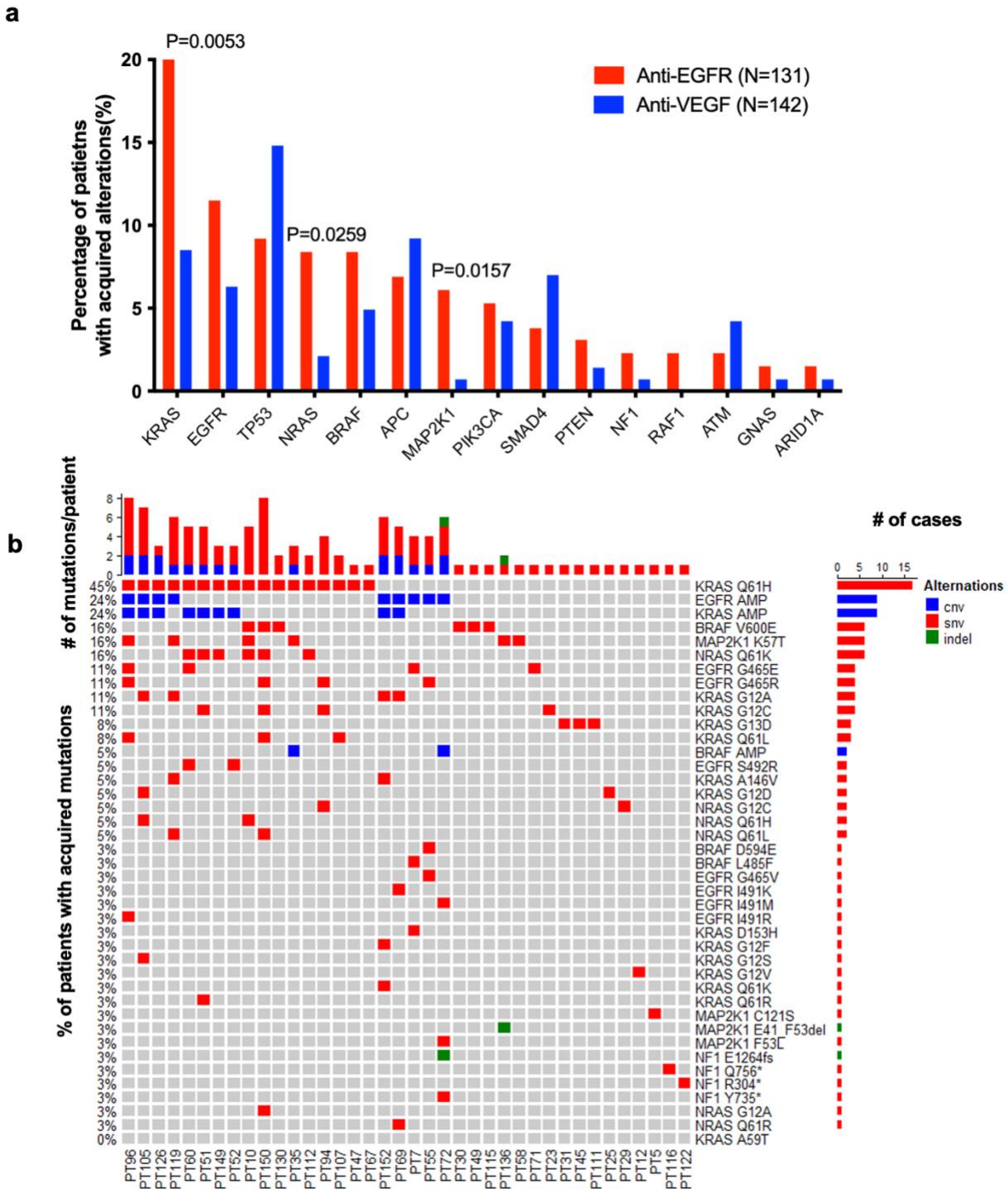

Supplementary Fig. 4. Comparison of genomic alterations detected in mCRC patients with Guardant360 ctDNA tests both prior to and after anti-EGFR (N=131) or anti-VEGF (N= 142) treatment. (a). Comparison of percentage of patients with gene-level acquired alterations between patients receiving anti-EGFR therapies and anti-VEGF therapies. (b) Acquired

EGFR/MAPK pathway alterations detected in anti-EGFR treated patients with each column representing an individual patient. The bar graph on the top of the oncoPrint represents the total number of acquired alterations detected in each individual patient. The numbers on the left side of the oncoPrint represent the percentage of patients with the specific acquired alteration listed on the right. The bar graph on the right of the oncoPrint represents the number of the patients with the specific acquired alterations listed on the left. Alterations that were absent from paired prior treatment but detected in post-treatment samples were defined as acquired alterations. Only oncogenic snv/indel/fusion and medium or high level of CNV in given genes were considered for this analysis. For the percentage of patients with gene-level acquired alterations, only those without any alterations in the specified gene detected in prior treatment samples but detected in post treatment samples will be considered. *P* value determined by two-tailed Fisher's exact Test. Source data for panels a and b are provided as a Source Data file.

Supplementary Figure 5

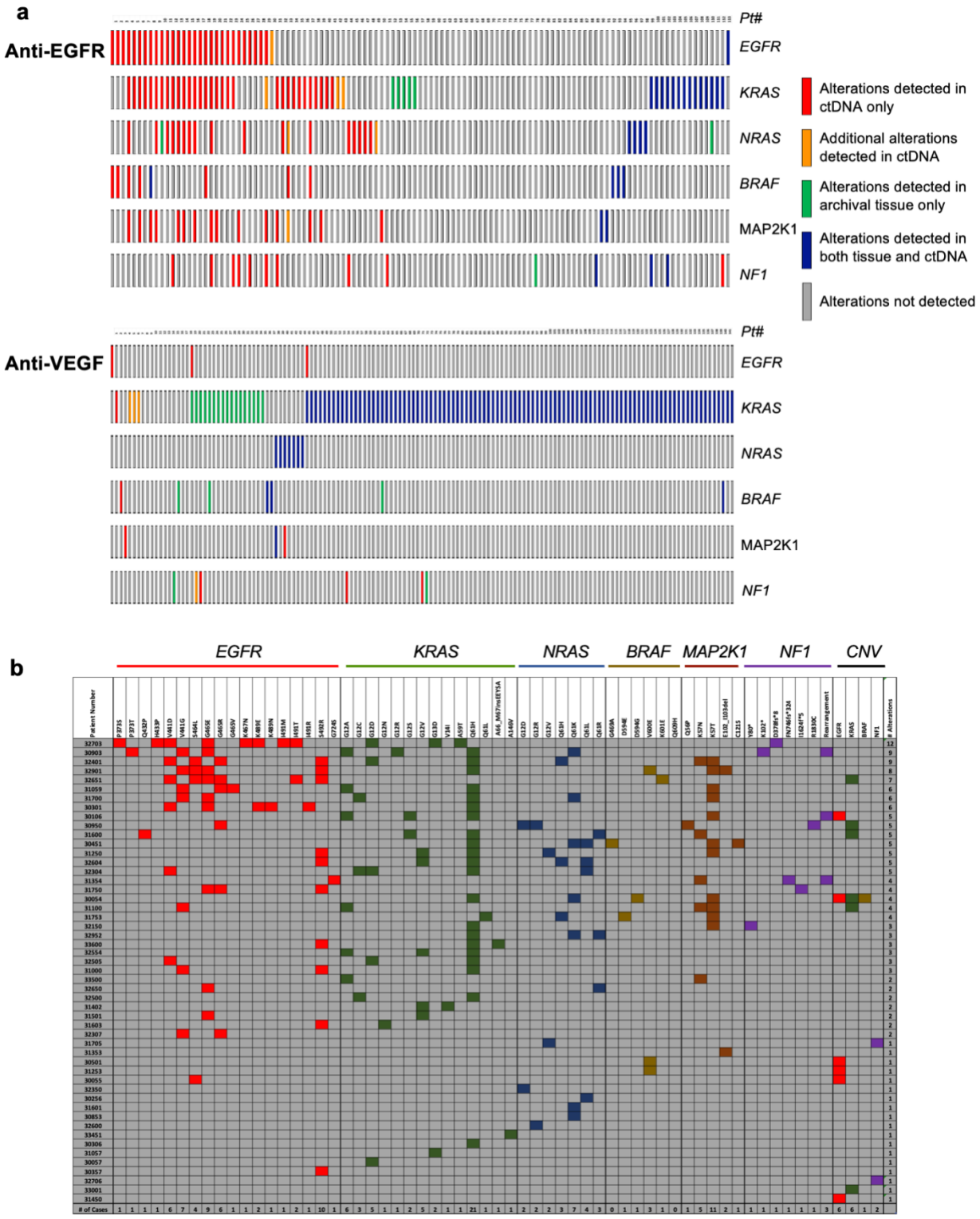

Supplementary Fig. 5. Identification of multiple EGFR/MAPK pathway activating alterations in IMblaze370 study individual patients following anti-EGFR therapies. (a), Comparison of EGFR/MAPK pathway gene-level alterations identified in paired plasma samples versus tumor tissue samples with each pair of bars. Bars in the same column represent an individual patient. Top, Alterations detected in patients that received prior anti-EGFR therapies(N=113). Bottom, alterations detected in patients that received prior anti-VEGF therapies(N=141). Red represents alterations identified in plasma but not in tumor tissue. Orange represents additional alterations identified in plasma. Green represents alterations identified in tumor tissue but not in plasma. Blue represents alterations identified in both plasma and tumor tissue. Gray represents no alterations detected in either plasma or tumor tissue. (b), Emerging EGFR/MAPK pathway activation alterations detected in plasma for patients who received prior anti-EGFR therapies with each row representing an individual patient. The numbers listed on the right represent the total number of emerging alterations detected in each individual patient. The numbers listed on the bottom represent the number of cases with specific emerging alterations detected in anti-EGFR treated patients. Only Known and likely pathogenic alterations in each gene were considered for the analysis. Source data for panels a and b are provided as a Source Data file.

Supplementary Figure 6

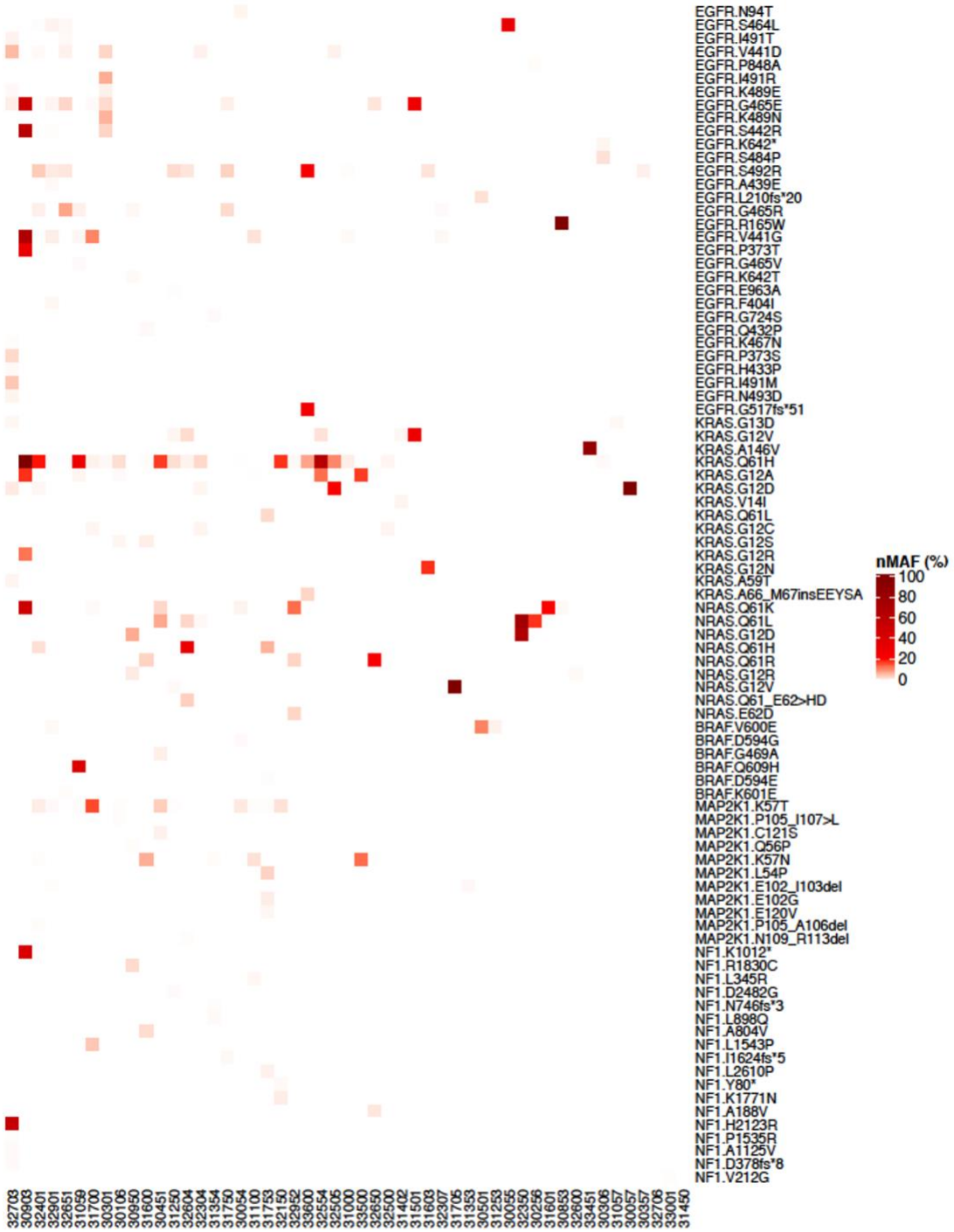

Supplementary Fig. 6. Heatmap shows normalized mutation allele frequency (nMAF) values of multiple acquired allele mutations of EGFR/MAPK pathways genes detected at the baseline plasma samples of the anti-EGFR treated IMblaze370 patients with (N= 51). Source data are provided as a Source Data file.

Supplementary Figure 7

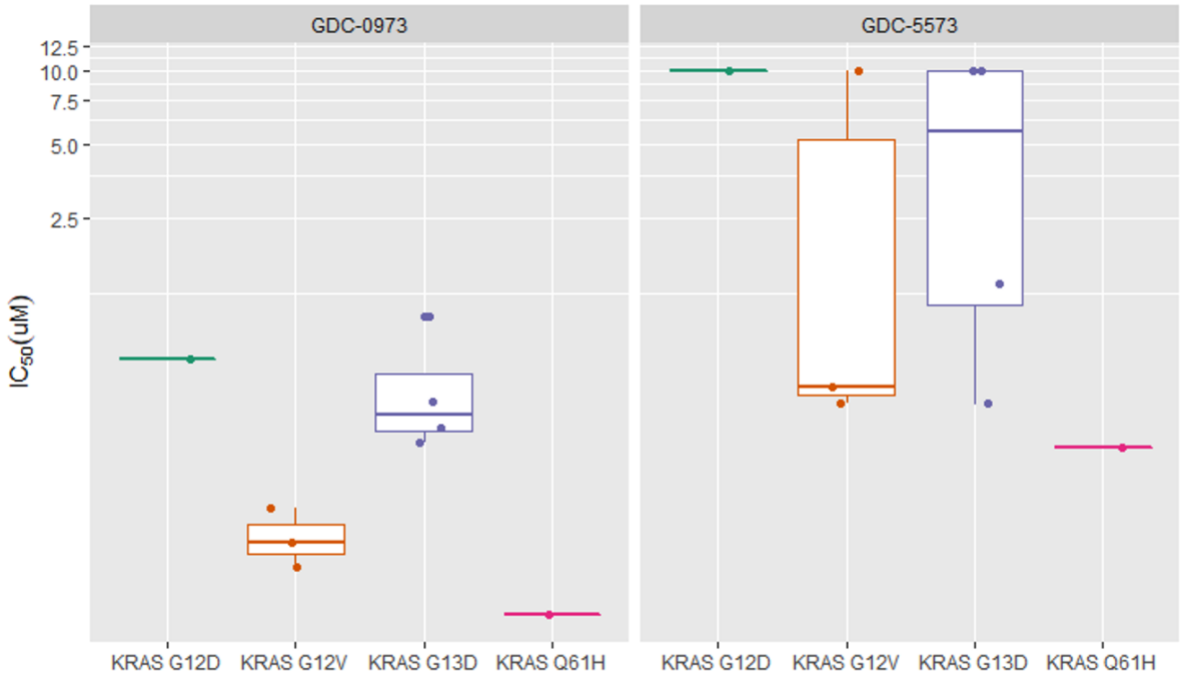

Supplementary Fig.7. Comparison of relative viability of KRAS^{Q61H} CRC cell line with KRAS^{G12D}, KRAS^{G12V}, and KRAS^{G13D} CRC cell lines in response to MEK inhibitor GDC-0973 and pan-RAF inhibitor GDC-5573 treatment. The reported IC_{50} is the dose at which the estimated inhibition is 50% relative to untreated wells. The bar indicated the median. Source data are provided as a Source Data file.

Supplementary Figure 8

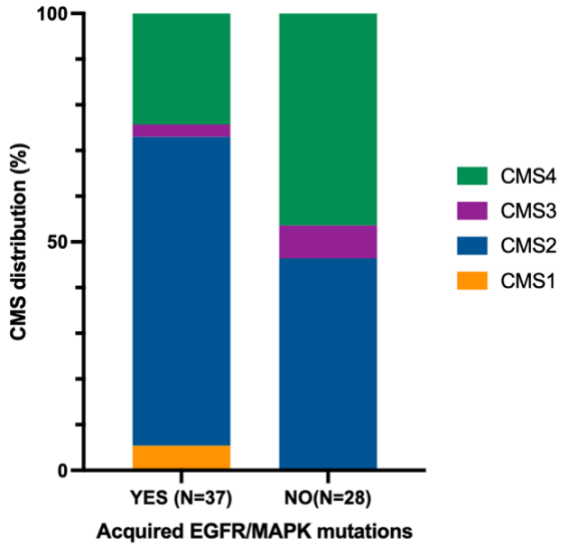

Supplementary Fig. 8. The distribution of four CMS subtypes in anti-EGFR treated IMblaze 370 patients with acquired EGFR/MAPK pathway gene alterations (N=37) and patients without acquired alterations (N=28). Source data are provided as a Source Data file.

Supplementary Figure 9

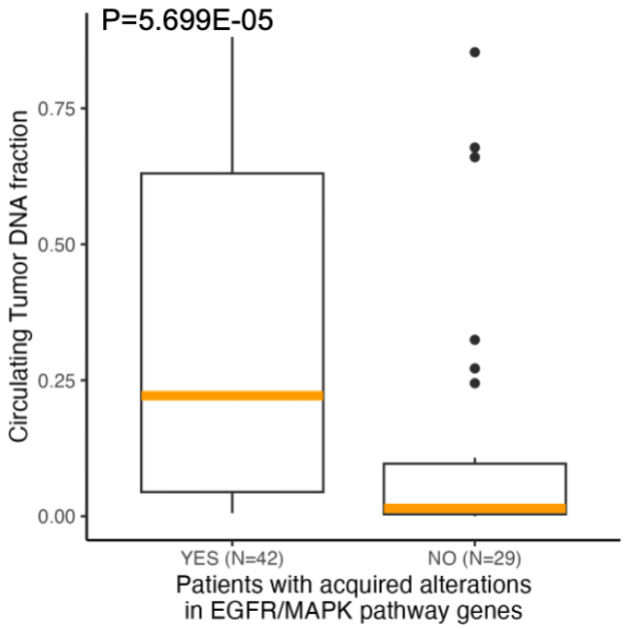

Supplementary Fig. 9. Comparison of estimated circulating tumor DNA fraction between anti-EGFR treated patients with acquired mutations in EGFR/MAPK genes (N=42) and those without (N=29) from IMblaze370 study. The bar indicated the median, while the edges of the box represent the IQR. The whiskers extend from the box to the farthest data point lying within 1.5x the inter-quartile range (IQR) from the box. Flier points are those past the end of the whiskers. P value determined using a 2-tailed Mann-Whitney U test. Source data are provided as a Source Data file.

Supplementary Figure 10

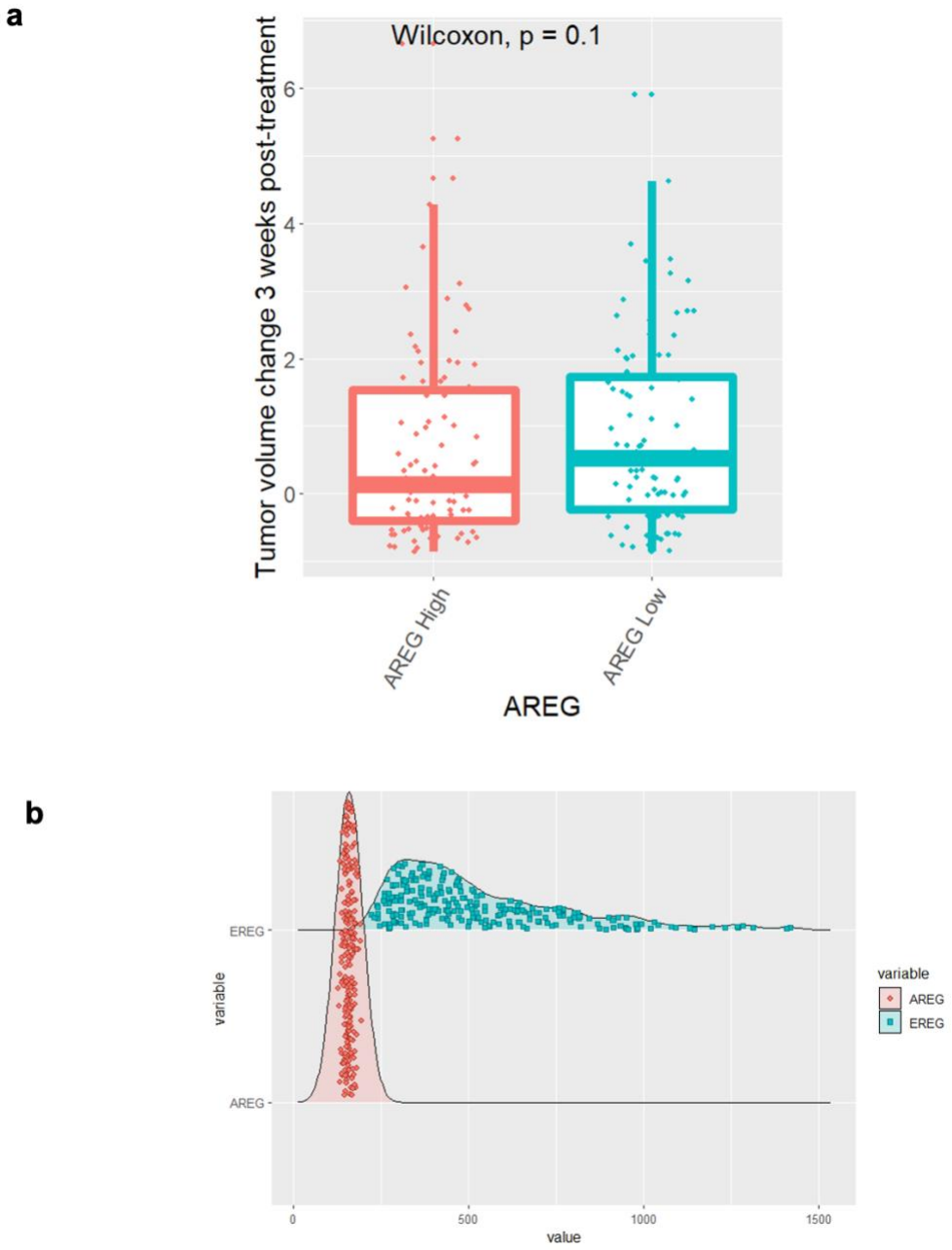

Supplementary. Fig. 10. Correlation of AREG expression and Cetuximab response in PDX models. (a) Changes in tumor volume from baseline to 3 weeks post cetuximab treatment in 244 PDX models with AREG high (above median, n=122) and *AREG* low (below median, n=122) tumors. The box and whisker plot shows the median, quartiles (hinges), whiskers, and individual outliers. *P* value determined using a two-sided Wilcoxon rank sum test. (b) Ridge plot showing the distribution of the expression levels of *EREG* and *AREG* in 244 PDX models. Source data for panels a and b are provided as a Source Data file.

Supplementary Table 1

Amplicon	# Anti-EGFR	# Amplicon Anti-EGFR	# Anti-VEGF	# Amplicon Anti-VEGF	OR	pval	FDR pval
8:46000001:147000000	113	21	141	9	3.3478	0.003242	0.019454
13:18000001:116000000	113	18	141	15	1.5916	0.260486	0.620096
8:36000001:44000000	113	11	141	9	1.5817	0.355605	0.620096
20:1:63000000	113	27	141	27	1.3256	0.440602	0.620096
8:9000001:10000000	113	5	141	4	1.5856	0.516746	0.620096
8:34000001:35000000	113	4	141	5	0.9982	1	1

Supplementary Table 1. Association of amplicon alterations with anti-EGFR (N=113) and anti-VEGF (N=141) treatment groups in the IMblaze370 study. Alterations on chromosome 8q were significantly enriched in the anti-EGFR group (raw p=0.003; FDR-corrected p=0.02). A two-sided Fisher's exact test was used, with the FDR correction applied for multiple comparisons.

Supplementary Table 2

Delicon	# Anti-EGFR	# Delicon Anti-EGFR	# Anti-VEGF	# Delicon Anti-VEGF	OR	pval	FDR pval
20:55000001:63000000	113	8	141	2	5.2952	0.025529	0.153177
13:18000001:116000000	113	4	141	14	0.3329	0.052807	0.158422
20:20000001:21000000	113	7	141	3	3.0377	0.11467	0.22934
20:18000001:19000000	113	6	141	4	1.9206	0.347327	0.52099
8:1:42000000	113	9	141	12	0.9303	1	1
18:47000001:78000000	113	5	141	6	1.0417	1	1

Supplementary Table 2. Association of delicon alterations with anti-EGFR (N=113) and anti-VEGF (N=141) treatment groups in the IMblaze370 study. A trend toward 20q loss was observed in the anti-EGFR group (raw p=0.03; FDR-corrected p= 0.15), and 13q loss in the anti-VEGF (raw = 0.05, FDR-corrected p = 0.16). A two-sided Fisher's exact test was used, with the FDR correction applied for multiple comparisons.